

Polymeric Self-Assembled Monolayers. 5. Synthesis and Characterization of ω -Functionalized, Self-Assembled Diacetylenic and Polydiacetylenic Monolayers

Taisun Kim^{*,†}

Department of Chemistry, Hallym University,
Chuncheon, Kang-Won Do, 200-702, South Korea

Qi Ye and Li Sun^{*,‡}

Department of Chemistry, University of Minnesota, Minneapolis, Minnesota 55455-0431

Kwok C. Chan and Richard M. Crooks^{*,§}

Department of Chemistry, Texas A&M University, College Station, Texas 77843-3255

Received August 14, 1996[®]

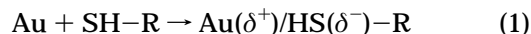
Here we discuss the preparation and characterization of photopolymerizable, self-assembled monolayers (SAMs) that consist of acid-, hydroxyl-, and methyl-terminated *n*-alkanethiols containing a diacetylene group (HS(CH₂)₁₀C≡CC≡C(CH₂)₁₀X; X = COOH, CH₂OH, and CH₃, respectively). The acid and hydroxyl surfaces are readily amenable to further synthetic elaboration, while the methyl-terminated SAM results in a clean, low-energy surface. As demonstrated by Fourier transform infrared external reflectance spectroscopy (FTIR-ERS), surface-enhanced Raman spectroscopy (SERS), ellipsometry, UV–vis spectroscopy, and electrochemical methods, all three materials self assemble onto Au surfaces to form ordered monolayers that can be photopolymerized with UV light.

Introduction

In this paper we discuss the preparation and characterization of photopolymerizable, self-assembled monolayers (SAMs) that consist of methyl-, hydroxyl-, and acid-terminated *n*-alkanethiols containing a diacetylene group. In previous papers in this series, we described the synthesis of the monomers¹ and showed that SAMs prepared from them can be used as ultrathin photoresists.² We have also shown that diacetylenic SAMs can be pillared by sequential polymerization and grafting steps to yield ordered, multilayer structures.³ In forthcoming papers we will discuss the viscoelastic and mechanical properties of the mono- and multilayers measured using thickness-shear mode resonators⁴ and interfacial force microscopy (IFM).^{5,6} We will also compare the stability of the polymerized and unpolymerized diacetylenic SAMs to that of simple *n*-alkanethiol SAMs and show that the polymerized materials are stable in aggressive solvents and at temperatures as high as 200 °C.⁷ However, we confine ourselves here to a comparison of the IR, Raman, and UV–vis spectroscopic, ellipsometric, and electrochemical properties of these materials.

Monolayer and multilayer self-assembly chemistry is useful for preparing well-ordered organic surfaces.^{8–11} A particularly popular and versatile version of monolayer self-assembly occurs when a Au substrate contacts a dilute vapor¹² or solution of a suitable organomercaptan.^{9,11,13} This treatment results in a surface-adsorbed monolayer possessing well-defined chemical and physical properties, which have been characterized by many analytical methods.^{9,11}

It is generally accepted that organomercaptan SAMs assume a ($\sqrt{3} \times \sqrt{3}$)R30° overlayer structure on Au(111) and that adsorption occurs at surface threefold hollow sites.^{9,14} Since many Au surfaces have a pronounced (111) texture, the ($\sqrt{3} \times \sqrt{3}$)R30° structure is often assumed to be common to all Au substrates, including vapor-deposited films and polycrystalline wires and foils. Organomercaptans are thought to interact with Au according to eq 1. The resulting Au(δ^+)/HS(δ^-)–R interaction has an



energy of about 44 kcal/mol, and the SAM is further stabilized by intermolecular van der Waals interactions.⁹ Spectroscopic studies indicate that methyl-terminated *n*-alkanethiol SAMs are composed of hydrocarbon chains tilted 30–40° from the surface normal and twisted ~50° about the carbon backbone. SAMs formed from shorter

* Authors to whom correspondence should be addressed.

† E-mail: tskim@sun.hallym.ac.kr.

‡ E-mail: sun@chemsun.chem.umn.edu.

§ E-mail: crooks@chemvx.tamu.edu.

® Abstract published in *Advance ACS Abstracts*, November 15, 1996.

(1) Kim, T.; Crooks, R. M. *Tetrahedron Lett.* **1994**, *35*, 9501.

(2) Chan, K. C.; Kim, T.; Schoer, J. K.; Crooks, R. M. *J. Am. Chem. Soc.* **1995**, *117*, 5877.

(3) Kim, T.; Crooks, R. M.; Tsen, M.; Sun, L. *J. Am. Chem. Soc.* **1995**, *117*, 3963.

(4) Shinn, N. D.; Michalske, T. A.; Martin, S. J.; Ricco, A. J.; Daly, C. L.; Krim, J.; Kim, T.; Yang, H. C.; Crooks, R. M. *Bull. Am. Phys. Soc.* **1996**, *41*, 609.

(5) Thomas, R. C.; Kim, T.; Crooks, R. M.; Houston, J. E.; Michalske, T. A. *J. Am. Chem. Soc.* **1995**, *117*, 3830.

(6) Thomas, R. C.; Houston, J. E.; Michalske, T. A.; Crooks, R. M. *Science* **1993**, *259*, 1883.

(7) Kim, T.; Chan, K. C.; Crooks, R. M. *J. Am. Chem. Soc.*, in press.

(8) Bigelow, W. C.; Pickett, D. L.; Zisman, W. A. *J. Colloid Sci.* **1946**, *1*, 513.

(9) Dubois, L. H.; Nuzzo, R. G. *Annu. Rev. Phys. Chem.* **1992**, *43*, 437 and references therein.

(10) Cao, G.; Hong, H.; Mallouk, T. E. *Acc. Chem. Res.* **1992**, *25*, 420.

(11) Ulman, A. *Introduction to Ultrathin Organic Films from Langmuir Blodgett to Self-Assembly*; Academic Press: New York, 1991.

(12) Chailapakul, O.; Sun, L.; Xu, C.; Crooks, R. M. *J. Am. Chem. Soc.* **1993**, *115*, 12459.

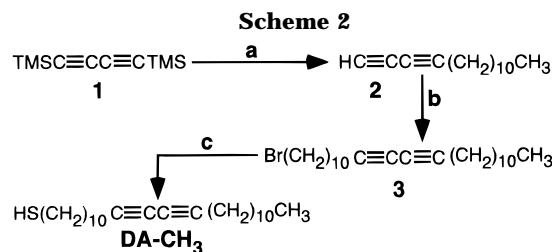
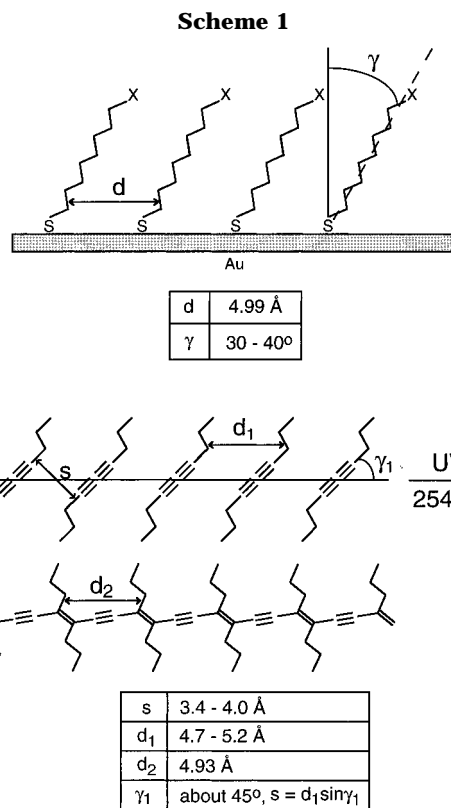
(13) Nuzzo, R. G.; Allara, D. L. *J. Am. Chem. Soc.* **1983**, *105*, 4481.

(14) Sun, L.; Crooks, R. M. *Langmuir* **1993**, *9*, 1951.

chains are typically, but not always,¹⁵ more disordered than those formed from longer chain molecules. Defects within ordered domains are thought to result primarily from gauche conformations within the lower energy all-trans, extended SAM structure. More significant defects arise at grain, rotational, and antiphase boundaries as well as at stacking faults.¹⁵

Polymerization of diacetylenes in the solid state was first reported by Wegner¹⁶ and has subsequently been discussed in detail by others.^{17–19} In contrast to the extended conjugation found in single crystals, alternative strategies, such as those based on Langmuir–Blodgett (LB) methods, usually result in conjugation defects.¹⁹ Cao and Mallouk have shown that the extent of polymerization of diacetylenic monomers in organometallic crystals depends on the coordinating metal ion; divalent metal ions yield polymers with the greatest extent of conjugation.^{10,20} Besides our own work, there has been one prior report of the polymerization of a monolayer prepared from methyl-terminated diacetylene disulfides.²¹ Studies such as these have yielded applications for polydiacetylenes as nonlinear optical materials,^{22,23} semiconductors and photoconductors,²⁴ drug delivery systems,²⁵ photolithographic resists,^{2,26} and chemical sensors.^{27,28} Finally, there have been several reports of SAMs that can be end-group polymerized using either electrochemical methods or light.^{29,30}

We designed and synthesized three different ω -functionalized diacetylenic (DA) *n*-alkanethiols: HS-(CH₂)₁₀C≡CC≡C(CH₂)₁₀X (X = COOH, DA-COOH; CH₂-OH, DA-OH; and CH₃, DA-CH₃). The acid^{3,31} and hydroxyl³² surfaces are readily amenable to further synthetic elaboration, while the methyl-terminated SAM results in a clean, low-energy surface. Scheme 1 illustrates the similarity between the lattice structure of Au-confined, *n*-alkanethiol SAMs (top) and the geometry of unpolymerized and polymerized diacetylene molecules (bottom).²⁰ The spacing between threefold hollow sites on the Au(111) surface is 4.99 Å. The organomercaptans that occupy these sites are tilted by about 30–40° with respect to the surface normal and twisted by ~50° (not shown) about the carbon backbone to maximize intermolecular van der Waals interactions.⁹ Unlike Langmuir and LB films, organomercaptans are strongly bound to their supporting surfaces and therefore are not expected to have the same degree of freedom to alter their conformation to accommodate polymerization. However, as illustrated in Scheme 1, the topochemical polymerization geometry is nearly



- a. 1 equiv of 1.5 M MeLi/LiBr, THF, -78 °C; Br(CH₂)₁₀CH₃/HMPA;
 b. 1 equiv of 1.6 M BuLi, THF, 0 °C; 5 equiv of Br(CH₂)₁₀Br/HMPA, rt;
 c. 6 equiv of NaSH/EtOH, 50–55 °C, 4 h, sonication

ideal, and little rearrangement should be required to yield linearly polymerized films if the diacetylenic thiols adopt a geometry on Au similar to that of *n*-alkanethiols.

Experimental Section

Chemicals. Most chemicals required for synthesizing the diacetylenes were of reagent-grade quality, purchased from Aldrich Chemical Co., and used without further purification. Anhydrous sodium hydrogen sulfide was obtained from Alfa Chemical and used as received. (3-Mercaptopropyl)trimethoxysilane was purchased from Hüls America Inc. (Bristol, PA). Water was purified (resistivity ≥ 18 M Ω -cm) using a Milli-Q reagent water system (Millipore).

Synthesis of Diacetylenic Alkanethiols. The syntheses of DA-COOH and DA-OH were discussed previously.¹ DA-CH₃ was synthesized *via* the same synthetic route using undecyl bromide instead of ω -(methoxymethoxy)alkyl bromide (Scheme 2).

1-Bromopentacos-11,13-diyne (3). To a stirred solution of **2** (10 mmol in 30 mL of THF), which was prepared from **1** and undecyl bromide in the presence of 1.5 M methyl lithium,¹ was added *n*-BuLi (5.9 mL, 1.6 M in hexane) at 0 °C. After 1 h, 1,10-dibromodecane (45 mmol, 13.5 g, 5 equiv) was added to the mixture as a solid, followed by addition of 10 mL of HMPA. The reaction mixture was stirred for an additional 30 min at 0 °C. The alkylated product was extracted from the mixture by 2 \times 200 mL of petroleum ether. The combined organic layers were washed with 2 \times 200 mL of water and dried over anhydrous sodium sulfate. Evaporation of solvent gave the crude product,

- (15) Poirier, G. E.; Tarlov, M. J. *Langmuir* **1994**, *10*, 2853.
 (16) Wegner, G. Z. *Naturforsch.* **1969**, *24b*, 824.
 (17) Lando, J. B. In *Polydiacetylenes*; Bloor, D., Chance, R., Eds.; Nijhoff: Dordrecht, The Netherlands, 1985.
 (18) Day, D. R.; Ringsdorf, H. *Makromol. Chem.* **1979**, *180*, 1059.
 (19) Wilson, T. E.; Ogletree, D. F.; Salmeron, M. B.; Bednarski, M. D. *Langmuir* **1992**, *8*, 2588 and references therein.
 (20) Cao, G.; Mallouk, T. E. *J. Solid State Chem.* **1991**, *94*, 59.
 (21) Batchelder, D. N.; Evans, S. D.; Freeman, T. L.; Haussling, L.; Ringsdorf, H.; Wolf, H. *J. Am. Chem. Soc.* **1994**, *116*, 1050.
 (22) Axon, T. L.; Bloor, D.; Molyneux, S.; Kar, A. K.; Wherrett, B. S. *Proc. SPIE* **1993**, *2025*, 374.
 (23) Winful, H. G.; Hartburger, J. H.; Garmire, E. *Appl. Phys. Lett.* **1979**, *35*, 379.
 (24) Day, D. R.; Lando, J. B. *J. Appl. Polym. Sci.* **1981**, *26*, 1605.
 (25) Koch, H.; Ringsdorf, H. *Makromol. Chem.* **1981**, *182*, 255.
 (26) Niederwald, H.; Seidel, H.; Güttler, W.; Schwoerer, M. *J. Phys. Chem.* **1984**, *88*, 1933.
 (27) Reichert, A.; Nagy, J. O.; Spevak, W.; Charych, D. *J. Am. Chem. Soc.* **1995**, *117*, 829.
 (28) Berman, A.; Ahn, D. J.; Lio, A.; Salmeron, M.; Reichert, A.; Charych, D. H. *Science* **1995**, *269*, 515.
 (29) McCarley, R. L.; Willicut, R. J. *J. Am. Chem. Soc.* **1994**, *116*, 10823.
 (30) Ford, J. F.; Vickers, T. J.; Mann, C. K.; Schlenoff, J. B. *Langmuir* **1996**, *12*, 1944.
 (31) Duevel, R. V.; Corn, R. M. *Anal. Chem.* **1992**, *64*, 337.
 (32) Sun, L.; Thomas, R. C.; Crooks, R. M.; Ricco, A. J. *J. Am. Chem. Soc.* **1991**, *113*, 8550.

which was purified by flash column chromatography (silica gel, petroleum ether) to give pure **3** in 23% yield. $^1\text{H NMR}$ (CDCl_3) δ : 3.400 (2H, t, $J = 6.8$ Hz), 2.235 (4H, t, $J = 6.8$ Hz), 1.848 (2H, m), 1.547–1.251 (32H, m), 0.873 (3H, t, $J = 6.4$ Hz).

1-Mercaptopentacosyl-11,13-diyne (DA-CH₃). Sodium hydrogen sulfide (NaSH , 0.6 mmol, 6 equiv) was added to a solution of alkyl bromide **3** (0.1 mmol) in absolute ethanol (4 mL), and the solution was degassed under Ar for 2 min. The reaction mixture was sonicated for 4 h at 50–55 °C, diluted with 3×10 mL of CH_2Cl_2 , and washed with acidic water (2–3 drops of 3 N HCl in 5 mL water) and 2×5 mL of DI water. The organic layer was dried over anhydrous sodium sulfate, and solvent was evaporated to give crude DA-CH₃. The crude mixture was recrystallized in 5 mL of hot hexane and subsequently filtered to give about a 65% yield of purified DA-CH₃ as a slightly yellow solid. $^1\text{H NMR}$ (CDCl_3) δ : 2.488 (2H, t, $J = 7.3$ Hz), 2.231 (4H, t, $J = 6.7$ Hz), 1.561–1.151 (34H, m), 0.872 (3H, t, $J = 6.5$ Hz).

NMR Spectroscopy. High-field NMR spectra were recorded on a Gemini or XL-200E spectrometer.

FTIR-External Reflectance Spectroscopy (FTIR-ERS). Substrate preparation for FTIR-ERS experiments was described previously.^{2,3} Briefly, about 2000 Å of Au was thermally or e-beam evaporated onto Ti- or Cr-primed (50–100 Å) Si(100) wafers. After the substrates were diced into 1.3×2.5 cm² pieces, they were cleaned in freshly prepared piranha solution (30% H_2O_2 /concentrated $\text{H}_2\text{SO}_4 = 1:3$). **Caution:** Piranha solution is a powerful oxidizing agent and reacts violently with organic compounds. It should be discarded immediately after use in a waste container with a loosely fitting lid.) for 15 s, rinsed, and dried. Monolayers were prepared by dipping freshly cleaned substrates into 1 mM THF or CHCl_3 solutions of the organo-mercaptans for 1 h or longer. Following deposition, the modified surfaces were rinsed with solvent and water (additionally, all acid-terminated SAMs were sonicated in 1.0 N HCl for 5 s and then rinsed with water) and then dried under flowing N_2 . Polymerization of the diacetylenic SAMs was performed by placing the substrate into a gas-tight polycarbonate container and irradiating it under a N_2 purge for up to 45 min (but typically 10 min) with a Hg(Ar) pencil-type UV lamp (Oriental, model 6035 (~1 W)), positioned 0.5–1 cm above the substrate.

FTIR-ERS spectra were acquired using a Digilab FTS-40 spectrometer (Bio-Rad, Cambridge, MA) equipped with a Harrick Scientific "Seagull" reflection accessory and a liquid-nitrogen-cooled MCT detector. All spectra were obtained using p-polarized light incident on the substrate at an angle of 84° with respect to the surface normal. All spectra were obtained at 2 cm⁻¹ resolution and are the sum of 256 individual spectra. Minimal baseline correction was applied to all spectra.

Raman Spectroscopy. The surface-enhanced Raman spectroscopy (SERS) measurement system was similar to that described previously³ with a slight modification: instead of the f-250 mm focusing lens, a $10\times$ microscope objective of 0.21 NA (Nikon) was used to focus the incident laser beam. The same objective was also used to collect the scattered Raman photons via a beam-splitting cube (Edmond Scientific, Barrington, NJ). Typical conditions for Raman scattering were 647.1 nm excitation (0.5 mW), 400 mm slit width (equivalent to a 14 cm⁻¹ bandpass), and 5 s integration time.

The electrochemical system for roughening Au substrates consisted of a bipotentiostat (model AFRDE5, Pine Instruments, Grove City, PA) which was computer-controlled via a programmable analog-digital interface board (model AT-MIO-16F-5, National Instruments, Austin, TX). To prepare the roughened Au substrate, a clean Au(111) facet was first obtained by melting and annealing an Au wire (99.9985%, 1.0 mm diameter, Johnson Matthey, Ward Hill, MA) in a H_2/O_2 flame.³³ The facet was then coated with an *n*-hexadecanethiol SAM prepared from a 1 mM ethanol solution. The defect sites within the SAM layer were utilized as nucleation sites on which SERS-active Au particles were electrochemically deposited at 0.3 V (vs Ag/AgCl, NaCl (3 M)) for 30 s from a solution containing 0.1 M HClO_4 and 1 mM HAuCl_4 . To enhance Au particle adhesion, the defect sites were intentionally etched at an electrode potential of 1.1 V prior to Au deposition. SERS-active Au particles prepared by this method can be readily characterized by scanning force microscopy. In this study, a relatively large particle size was chosen (greater than 1 μm) to minimize surface curvature. A detailed discussion

of this new type of SERS substrate will be provided in a forthcoming publication.³⁴ No effort was made to remove the *n*-hexadecanethiol SAM on the Au(111) surface, since its surface Raman scattering was below the limit of detection.

Immediately after it was rinsed with water and ethanol, the roughened Au substrate was immersed in a 1 mM diacetylene monomer solution of CHCl_3 for about 10 h, removed, rinsed with ethanol, and dried in a stream of N_2 . SERS from the diacetylenic SAM on the Au particles were measured in air. Polymerization under UV irradiation was achieved by placing the substrate 25 cm from a 30 W low-pressure Hg lamp (Conrad-Hanobia, NJ) for 10 min.

UV-vis Spectroscopy. Partially transmitting Au substrates for UV-vis measurements were prepared by thermal evaporation of 50 Å of Au onto both sides of (3-mercaptopropyl)trimethoxysilane-primed 1×2.5 cm² quartz substrates.^{35,36} The substrates were cleaned using a low-energy Ar plasma (Harrick Scientific Model PD6-32G) for 1 min. SAMs were prepared as described for the FTIR-ERS measurements. The UV-vis spectra (100 scans each, 2 nm resolution) were recorded on a Hewlett-Packard diode-array spectrometer (Model 8452A) by first obtaining a background spectrum of the unpolymerized diacetylenic SAM and then polymerizing it for various lengths of time without removing the substrate from the spectrometer. The UV light source was maintained 0.5–1.0 cm away from the substrate. Throughout these experiments the substrate was kept under a N_2 purge.

Ellipsometry. The substrates used to obtain ellipsometric thickness data were the same as those used for FTIR-ERS analysis. Thickness measurements of the polymerized and unpolymerized diacetylenic SAMs were made using a Gaertner Scientific ellipsometer (Model L116C). The data were obtained using the 488 nm Ar laser line, but the 633 nm He-Ne laser line yielded similar results. A refractive index of 1.46 was assumed for thickness calculations.

Electrochemical Measurements. Substrates for electrochemical measurements were prepared by thermal evaporation of 440 Å of Au onto (3-mercaptopropyl)trimethoxysilane-primed 1.0×2.5 cm² pieces of glass using methods similar to those discussed for the UV-vis substrates. Au substrates were cleaned for 1 min in an Ar plasma and then immediately immersed in a 1 mM THF solution of the diacetylenic thiol for at least 1 day. Prior to polymerization or electrochemical measurements, the substrates were rinsed with THF and water. Diacetylenic SAMs were polymerized identically to those prepared for the FTIR-ERS experiments.

A single-compartment electrochemical cell containing the Au working electrode (immersed electrode area = 0.7 cm²), a reference electrode (Ag/AgCl, NaCl (3 M)), and a Pt counter electrode was used to obtain cyclic voltammetric data. Capacitance measurements were carried out in an aqueous 0.1 M KCl electrolyte solution (scan rate = 100 mV/s), and Faradaic electrochemical experiments were performed in a 0.1 M KCl electrolyte solution containing 5 mM $\text{Ru}(\text{NH}_3)_6\text{Cl}_3$ (scan rate = 50 mV/s).

Results and Discussion

Raman Spectroscopy. Figure 1 shows the SERS spectra of UV-polymerized SAMs of DA-COOH, DA-OH, and DA-CH₃ on roughened Au surfaces. The resemblance of the three spectra is not surprising, since their principal bands originate from vibrations of the polydiacetylene (PDA) backbone, which contains conjugated and alternating C=C and C≡C bonds.³ The normal modes of several PDAs have been analyzed on the basis of bulk Raman spectra using a simplified model containing only five independent force constants.^{37,38} According to this model, the peaks around 1444 and 2075 cm⁻¹ can be assigned to

(34) Xiao, T.; Ye, Q.; Sun, L. Submitted for publication in *J. Phys. Chem.*

(35) Goss, C. A.; Charych, D. H.; Majda, M. *Anal. Chem.* **1991**, *63*, 85.

(36) DiMilla, P. A.; Folkers, J. P.; Biebuyck, H. A.; Haerter, R.; Lopez, G. P.; Whitesides, G. M. *J. Am. Chem. Soc.* **1994**, *116*, 2225.

(37) Bloor, D.; Preston, F. H.; Ando, D. J.; Batchelder, D. N. In *Structural Studies of Macromolecules by Spectroscopic Method*; Iven, K. J., Ed.; John Wiley & Sons: London, 1976; Chapter 8.

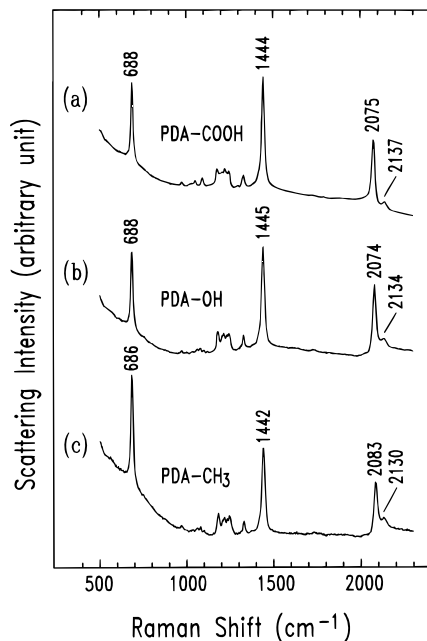


Figure 1. SERS spectra for SAMs of (a) DA-COOH, (b) DA-OH, and (c) DA-CH₃ on roughened Au surfaces after 10 min irradiation with UV light.

the C=C and C≡C stretching vibrations, respectively. Because of the extensive electronic delocalization in the PDA backbone these frequencies are lower than those for isolated C=C and C≡C bonds (1620 and 2260 cm⁻¹, respectively).^{39,40} The remaining prominent peak around 687 cm⁻¹ is due to an in-plane bending mode of the backbone, but this assignment is less definitive due to its low frequency and the uncertainty of the force constants used in the model.

The peak positions of the C=C and C≡C stretching vibrations agree with those observed in previous studies.^{3,21,41,42} For example, Batchelder et al. detected two bands at 1455 and 2074 cm⁻¹ from a polymerized diacetylenic SAM on smooth Au.²¹ Chen et al. reported SERS bands at 1456 and 2078 cm⁻¹ from the polymerized LB film of a similar diacetylene on Ag island films.⁴¹ These peak positions suggest, and UV-vis spectroscopic data discussed later confirm, that the polymerized DA films exist in a structurally ordered "blue" phase.³⁸ In contrast, the less ordered "red" phase would show bands around 1517 and 2115 cm⁻¹ according to a previous study on LB films of PDA.⁴² We have observed a weak band around 2135 cm⁻¹, which may indicate the presence of a small fraction of the red phase. However, this peak should be accompanied by the one around 1517 cm⁻¹, which is assigned to the C=C stretching mode of the red phase, and it is not.

Besides low-power, UV-induced polymerization, a DA monolayer can also be polymerized by the incident laser light at 647.1 nm. This result agrees with those of Batchelder et al., who observed that a He-Ne laser at 632.8 nm initiated polymerization,²¹ and of Angkaew et al., who observed similar phenomena using a 750.7 nm

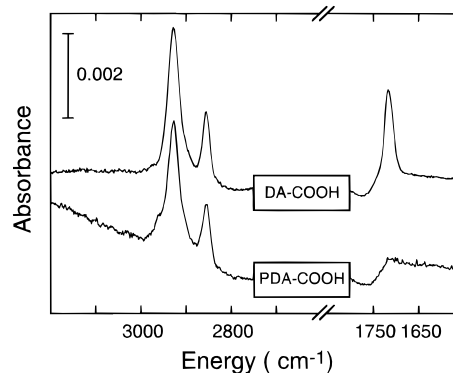


Figure 2. FTIR-ERS spectra of a HS(CH₂)₁₀C≡CC≡C(CH₂)₁₀-COOH SAM-modified Au surface before (DA-COOH) and after (PDA-COOH) UV-light-induced polymerization.

titanium-sapphire laser.³⁹ We found that the rate of laser-induced polymerization increases as the laser power density increases. With the present experimental setup, a large power density is produced by focusing the laser beam with the 10× microscope objective. As a result, the polymerization can be initiated with a power as low as 0.2 mW. SERS spectra of laser-induced PDA monolayers are very similar to those obtained after UV irradiation except for a subtle difference: the peak due to the C≡C stretching vibration, which occurs at 2075 cm⁻¹ after UV-induced polymerization, is located 2–6 cm⁻¹ lower when polymerization is laser induced. This may be explained by the strain theory of Batchelder et al. who concluded that the C≡C stretching frequency decreases as the internal crystal strain increases.^{38,43} Since laser-induced polymerization is likely to be incomplete, a higher crystal strain within the two-dimensional monolayer lattice is expected, which leads to a lower C≡C stretching frequency.³⁸ In contrast, the fractional conversion from DA to PDA after UV irradiation should be higher than that without UV irradiation, resulting in lower strain and higher stretching frequency. The internal strain is relaxed completely when all the DA is converted to PDA.

No SERS from an unpolymerized DA monolayer can be detected. The failure to detect the C≡C bonds in the DA monolayer may be attributed to the large distance between these bonds and the Au surface.⁴⁴ It is surprising, however, that we did not detect SERS from the C-S stretching vibration, which is closer to the surface and which has been observed previously.⁴⁵ We do not fully understand this observation other than noting that the surface morphology of the roughened Au substrate and collection optics may not have been sufficiently well optimized to detect this band or others resulting from vibrations of the methylene skeleton. In comparison, detection of the PDA backbone is possible because of the additional resonance enhancement. As discussed later, the blue form of PDA has an intense absorption band near 620 nm that encompasses the 647.1 nm laser line. The resonance enhancement mechanism is well supported by many previous studies of Raman scattering from PDA single crystals, which indicate that the Raman excitation profile follows closely the absorption profile.³⁸

FTIR-ERS. Figure 2 shows FTIR-ERS spectra of a HS(CH₂)₁₀C≡CC≡C(CH₂)₁₀COOH SAM before (DA-COOH) and after (PDA-COOH) polymerization by UV light. Prior to polymerization, the DA-COOH spectrum reveals two high-energy absorptions at 2930 and 2856 cm⁻¹ that arise from asymmetric ($\nu_a(\text{CH}_2)$) and symmetric ($\nu_s(\text{CH}_2)$) me-

(38) Batchelder, D. N.; Bloor, D. In *Advances in Infrared and Raman Spectroscopy*; Clark, R. J. H., Hester, R. E., Eds.; Wiley Heyden: London, 1984; pp 133–209.

(39) Angkaew, S.; Wang, H.-Y.; Lando, J. B. *Chem. Mater.* **1994**, *6*, 1444.

(40) Lin-Vien, D.; Colthup, N. B.; Fateley, W. G.; Grasselli, J. G. In *The Handbook of Infrared and Raman Characteristic Frequencies of Organic Molecules*; Academic Press: San Diego, CA, 1991.

(41) Chen, Y. J.; Carter, G. M.; Tripathy, S. K. *Solid State Commun.* **1985**, *54*, 19.

(42) Burzynski, R.; Prasad, P. N.; Biegajski, J.; Cadenhead, D. A. *Macromolecules* **1986**, *19*, 1059.

(43) Bloor, D.; Dennedy, R. J.; Batchelder, D. N. *J. Polym. Sci.: Polym. Phys. Ed.* **1979**, *17*, 1355.

(44) Tsen, M.; Sun, L. *Anal. Chim. Acta* **1995**, *307*, 333.

(45) Bryant, M. A.; Pemberton, J. E. *J. Am. Chem. Soc.* **1991**, *113*, 8284.

Table 1. FTIR-ERS Peak Assignments of DA-COOH, MUA, DA-OH, MUD, and DA-CH₃ before and after Exposure to UV Light

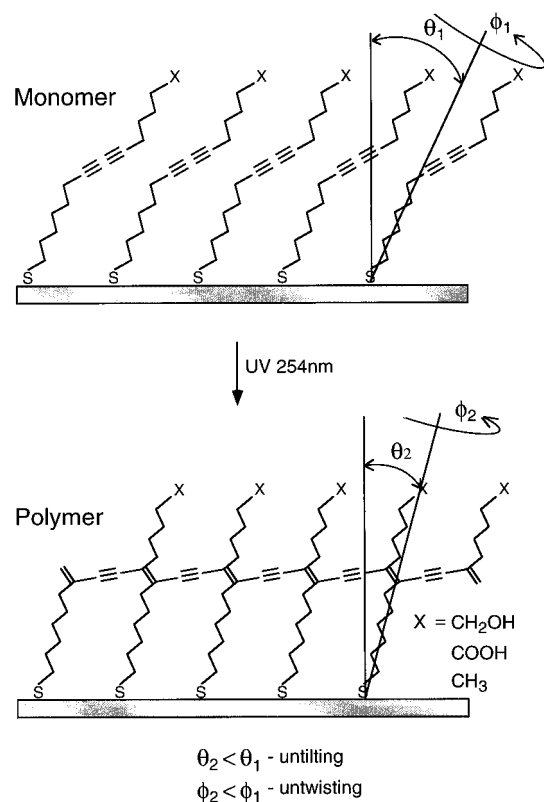
	$\nu_s(\text{CH}_2)/$ (fwhm), cm^{-1}	$\nu_a(\text{CH}_2)/$ (fwhm), cm^{-1}	$\nu(\text{C}=\text{O})/$ (fwhm), cm^{-1}
Figure 2—DA-COOH			
before UV	2856/(18)	2930/(32)	1719/(26)
after UV	2856/(20)	2926/(29)	1719/(58)
Figure 3—MUA			
before UV	2856/(21)	2926/(29)	1719/(19)
after UV	2856/(20)	2926/(27)	1719/(20)
Figure 4—DA-OH			
before UV	2856/(18)	2927/(32)	<i>a</i>
after UV	2858/(18)	2928/(34)	<i>a</i>
Figure 5—MUD			
before UV	2854/(17)	2924/(30)	<i>a</i>
after UV	2856/(23)	2922/(28)	<i>a</i>
Figure 6—DA-CH ₃			
before UV	2857/(15)	2927/(27)	<i>a</i>
after UV	2856/(15)	2926/(35)	<i>a</i>

^a Values not determined.

thylene stretching modes, respectively (the FTIR-ERS data are summarized in Table 1). The positions of these bands indicate that the hydrocarbon backbones are not structurally ordered as they are in SAMs prepared from *n*-alkanes, which have methylene bands at lower energies ($\nu_a(\text{CH}_2) = 2918 \text{ cm}^{-1}$ and $\nu_s(\text{CH}_2) = 2851 \text{ cm}^{-1}$).⁴⁶ The rigid, rodlike diacetylene groups present in the middle of the lattice structure are probably responsible for the decreased packing efficiency of the chains.⁴⁷ In addition to the methylene modes, there is also a single, strong absorption at 1719 cm^{-1} arising from the C=O of the carboxylic acid terminal group. The position of this band suggests that the acid groups undergo lateral hydrogen bonding in analogy to acid-terminated alkanethiols.^{48,49} The ellipsometrically measured thickness of the DA-COOH SAM is $24 \pm 2 \text{ \AA}$. Because the length of extended, all-trans DA-COOH is about 32 \AA ,⁵⁰ we infer that alkyl chains are tilted an average of about 42° from the surface normal prior to polymerization.

The lower spectrum in Figure 2 shows the spectral changes attendant upon polymerization of DA-COOH. The PDA-COOH $\nu_a(\text{CH}_2)$ band decreases in magnitude by about 30%, shifts to lower energy (2926 cm^{-1}), and sharpens slightly ($\Delta\text{fwhm} = -3 \text{ cm}^{-1}$), which suggest that polymerization causes an orientational change in the alkyl chains and improves their ordering. The $\nu_s(\text{CH}_2)$ band also decreases in magnitude, but its position does not change. Finally, a very small shoulder appears on the high-energy side of the $\nu_a(\text{CH}_2)$ band, which is consistent with CH₃ contamination of the polymerized SAM. This band is also present in spectra of acid- and hydroxyl-terminated *n*-alkanethiol SAMs following exposure to UV light (*vide infra*). The presence of hydrocarbon contamination on these active surfaces is not surprising.

The position of the C=O band remains unchanged at 1719 cm^{-1} after polymerization, suggesting that the acid groups remain hydrogen bonded after polymerization, but the magnitude decreases dramatically, which strongly

Scheme 3

suggests a significant change in end-group orientation.⁵¹ As for the DA-COOH SAM, the measured ellipsometric thickness of the PDA-COOH SAM is about 24 \AA . That there is no difference between the thicknesses of the DA and PDA SAMs is the result of a fortuitous cancellation of effects: although the SAMs untilt somewhat after polymerization, the individual molecules that comprise the SAM are actually somewhat shorter following polymerization.⁵⁰

In FTIR-ERS, vibrations are active only if there is a change in the dipole-moment vector component normal to the surface and then the absorbance is proportional to the square of that component dipole-moment change. Spectral differences before and after polymerization are suggestive of molecular reorganization.⁵² For the asymmetric and symmetric CH₂ modes to be active, DA-COOH must be both tilted (relative to the surface normal) and twisted (about the alkyl backbone), as shown in Scheme 3.⁵²

After polymerization, we observed that the absorbance of the CH₂ peaks decreases. Since there are no chemical changes in the CH₂ groups during polymerization, the decrease in absorbance must result from the untilting and untwisting of the alkyl chains relative to the initial DA-COOH configuration (bottom panel of Scheme 3). A similar argument can be applied to the C=O band at 1719 cm^{-1} . Before polymerization, the C=O group, which has a dipole moment along the C=O bond, is oriented somewhat vertically with respect to the Au surface. After polymerization, the C=O absorbance decreases dramatically, implying that the C=O group in PDA-COOH is nearly parallel to the surface.

We were concerned that UV exposure, which is used to polymerize the SAMs, could damage or otherwise change the chemical or structural characteristics of the PDA-COOH SAMs. For example, it has been shown that UV

(46) Porter, M. D.; Bright, T. B.; Allara, D. L.; Chidsey, C. E. D. *J. Am. Chem. Soc.* **1987**, *109*, 3559.

(47) Evans, S. D.; Urankar, E.; Ulman, A.; Ferris, N. *J. Am. Chem. Soc.* **1991**, *113*, 4121.

(48) Sun, L.; Crooks, R. M.; Ricco, A. J. *Langmuir* **1993**, *9*, 1775.

(49) Sun, L.; Kepley, L. J.; Crooks, R. M. *Langmuir* **1992**, *8*, 2101.

(50) In ref 3 we estimated the length of DA-COOH and PDA-COOH molecules to be 30 and 28 Å, respectively, but using computer modeling methods (InsightII, Biosym), we have refined these values slightly. The correct lengths of all-trans, extended DA-COOH and PDA-COOH are 32 and 30 Å, respectively.

(51) Wilson, E. B., Jr.; Decius, J. C.; Cross, P. C. *Molecular Vibrations*; Dover: New York, 1955; p 43.

(52) Nuzzo, R. G.; Dubois, L. H.; Allara, D. L. *J. Am. Chem. Soc.* **1990**, *112*, 558.

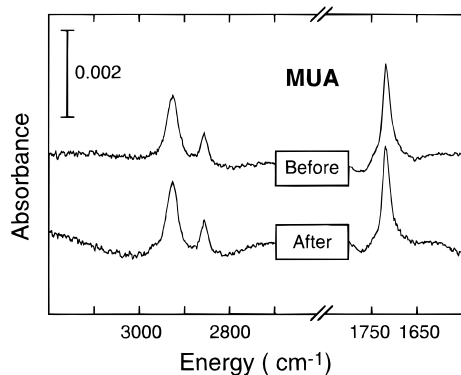


Figure 3. FTIR-ERS spectra of a HS(CH₂)₁₀COOH (MUA) SAM-modified Au surface before and after UV irradiation.

illumination in the presence of air leads to photooxidation of sulfur in *n*-alkanethiols and renders such SAMs easily removed from the Au substrate.^{53,54} To ensure that such destabilization does not occur for PDA-COOH and that the spectral changes noted above arise only from structural changes attendant upon polymerization, we exposed a SAM composed of mercaptoundecanoic acid (MUA) to UV light under exactly the same conditions used to polymerize the DA-COOH SAM. The FTIR-ERS results of this experiment are shown in Figure 3. Before exposure to UV light, methylene stretching bands are present at $\nu_a(\text{CH}_2) = 2926 \text{ cm}^{-1}$ and $\nu_s(\text{CH}_2) = 2856 \text{ cm}^{-1}$,⁵⁵ and a strong C=O absorption occurs at 1719 cm^{-1} , as we observed for the DA-COOH and PDA-COOH SAMs. It has been previously noted that the MUA C=O band actually consists of two poorly resolved components at about 1739 and 1718 cm^{-1} , corresponding to nonhydrogen-bonded and laterally hydrogen-bonded acid groups, respectively.^{48,49,56} We previously found that when MUA SAMs are rinsed in neutral water, the pH is not sufficiently low to yield full protonation; therefore, in this experiment we exposed them (and all other acid-terminated SAMs) to aqueous acid prior to analysis to ensure full protonation. This treatment causes the higher energy C=O band to be replaced by the single peak shown in Figure 3. This effect is fully reproducible.

The important point of these experiments is that, under the conditions used here, illumination does not change the MUA SAM: the magnitudes of the peaks, their fwhm, and their positions are identical, within spectral resolution, before and after exposure to UV light. This result contrasts sharply with those reported by Hemminger⁵³ and Tarlov;⁵⁴ however, the experiments reported here were performed in the absence of O₂. This control experiment demonstrates that the conditions used for DA-COOH polymerization do not undermine the structural integrity of the SAMs and that the spectral changes shown in Figure 2 are associated only with polymerization.

Hydroxyl (HS(CH₂)₁₀C≡CC≡C(CH₂)₁₀OH)- and methyl (HS(CH₂)₁₀C≡CC≡C(CH₂)₁₀CH₃)-terminated diacetylene molecules (DA-OH and DA-CH₃, respectively) also yield

(53) Huang, J. Y.; Hemminger, J. C. *J. Am. Chem. Soc.* **1993**, *115*, 3342.

(54) Tarlov, M. J.; Burgess, D. R. F.; Gillen, G. *J. Am. Chem. Soc.* **1993**, *115*, 5305.

(55) The $\nu_a(\text{CH}_2)$ and $\nu_s(\text{CH}_2)$ energies are both about 6 cm^{-1} higher than we reported previously for MUA (see refs 48, 49, and 56). This apparent discrepancy arises from a structural change that occurs during aging of the films. In previous studies we always measured the IR spectrum immediately after forming the SAM, but all the acid-terminated films discussed here were aged for periods of up to 2 days prior to spectral acquisition. The shift in the methylene bands in the acid-terminated SAMs (only) upon aging is a fully reproducible effect and probably reflects relaxation of the hydrocarbon chains.

(56) Yang, H. C.; Dermody, D. L.; Xu, C.; Ricco, A. J.; Crooks, R. M. *Langmuir* **1996**, *12*, 726.

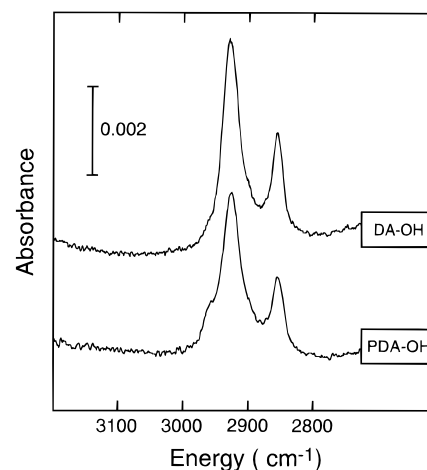


Figure 4. FTIR-ERS spectra of a HS(CH₂)₁₀C≡CC≡C(CH₂)₁₀-CH₂OH SAM-modified Au surface before (DA-OH) and after (PDA-OH) UV-light-induced polymerization.

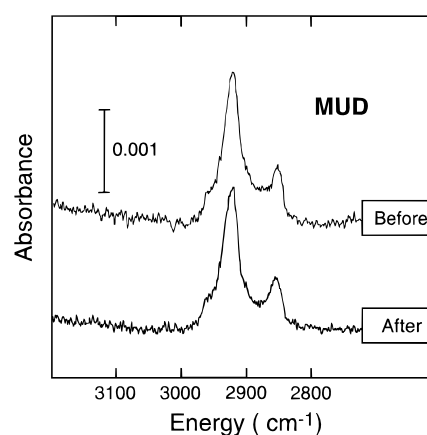


Figure 5. FTIR-ERS spectra of a HS(CH₂)₁₀CH₂OH (MUD) SAM-modified Au surface before and after UV irradiation.

polymerized SAMs (PDA-OH and PDA-CH₃, respectively) upon exposure to UV light. FTIR-ERS spectra of DA-OH and PDA-OH SAMs are shown in Figure 4. The $\nu_a(\text{CH}_2)$ and $\nu_s(\text{CH}_2)$ bands are present at 2927 and 2856 cm^{-1} , respectively, but upon polymerization these bands decrease in intensity by about 25% and their positions are unchanged. The $\nu(\text{OH})$ band centered around 3300 cm^{-1} is broad and poorly defined before and after polymerization. These results are in general agreement with the DA-COOH/PDA-COOH system discussed earlier, and they suggest that the DA-COOH SAM undergoes a small but significant structural change upon polymerization. To ensure that UV illumination does not destabilize the PDA-OH SAM, we performed a control experiment analogous to the MUA experiment discussed earlier (Figure 5). The results indicate that SAMs prepared from 11-mercaptoundecanol (MUD) do not undergo significant spectral changes upon UV irradiation.

FTIR-ERS data for SAMs prepared from the methyl-terminated diacetylene are shown in Figure 6. Prior to polymerization, the spectrum of DA-CH₃ reveals $\nu_a(\text{CH}_2)$ and $\nu_s(\text{CH}_2)$ bands at 2927 and 2857 cm^{-1} , respectively, and the $\nu_a(\text{CH}_3)$ band is present at 2962 cm^{-1} . Upon polymerization, the bands do not shift but their magnitude decreases by about 15%, indicating they undergo small but significant structural changes upon polymerization.

UV-vis Spectroscopy. Upon polymerization, diacetylenic SAMs absorb visible light. The optical properties of single crystals of PDA have been extensively

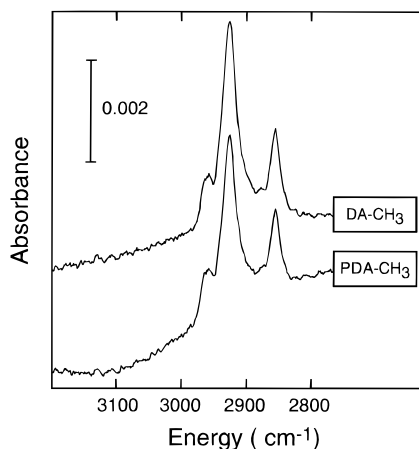


Figure 6. FTIR-ERS spectra of a $\text{HS}(\text{CH}_2)_{10}\text{C}\equiv\text{CC}\equiv\text{C}(\text{CH}_2)_{10}\text{-CH}_3$ SAM-modified Au surface before (DA- CH_3) and after (PDA- CH_3) UV-light-induced polymerization.

studied.⁵⁷ The carbon backbone of fully conjugated PDA is planar, and the lowest energy optical transition ($\pi-\pi^*$) is typically located at about 620 nm. Therefore, fully conjugated PDA absorbs red light and appears as a blue polymer. However, distortion of the conjugated carbon backbone due to disorder or strain reduces the extent of orbital overlap and shortens the average conjugation length. This shifts the $\pi-\pi^*$ transition to a higher energy (~ 540 nm) and causes the polymer to appear red. Day and Ringsdorf¹⁸ reported a blue to red shift in the PDA absorption spectrum when they irradiated crystalline PDA with UV light for an extended period of time. The shift was attributed to a reorientation of the carbon backbone of the blue polymer, which effectively reduces the conjugation length and increases the energy of the optical transition.

Tieke and Lieser⁵⁸ studied the polymerization of LB films of diacetylenes having the general formula $\text{CH}_3(\text{CH}_2)_{m-1}\text{C}\equiv\text{CC}\equiv\text{C}(\text{CH}_2)_n\text{COOH}$. The color of the PDA LB films depends on the packing of the monomers. For well-packed films ($m = 12, n = 8$; $m = 10, n = 8$), the polymer is blue, indicating a high level of conjugation, but after extensive illumination it converts to the red polymer like the bulk-phase materials. For the less well-packed films ($m = 16, n = 2$; $m = 16, n = 0$), only the red polymer is obtained.

We exposed SAMs prepared from DA-COOH and DA-OH to UV light for varying lengths of time and measured the resulting optical spectra in the range 400–800 nm. The spectra at the top of Figure 7 show the spectral evolution of a DA/PDA-COOH SAM over a period of 13 min. After illuminating with UV light for 3 min, a very weak, broad absorbance having a wavelength maximum (λ_{max}) in the range 620–650 nm is apparent. As shown at the bottom of Figure 7, polymerization is complete after about 13 min, at which time there is a fairly well-developed peak present at 620 nm. On the basis of previous results obtained from DA/PDA crystals and LB films and the discussion of the resonance-enhanced Raman spectroscopy, we infer that there is a relatively high level of conjugation in the PDA SAMs. In contrast to results from PDAs in the solid state and in LB films, the PDA SAMs do not change into the red polymer even after extended UV illumination. We believe the conjugation stability of the PDA SAMs results from its strong interaction with the Au surface, which tends to reduce structural flexibility and impede reorientation after polymerization.

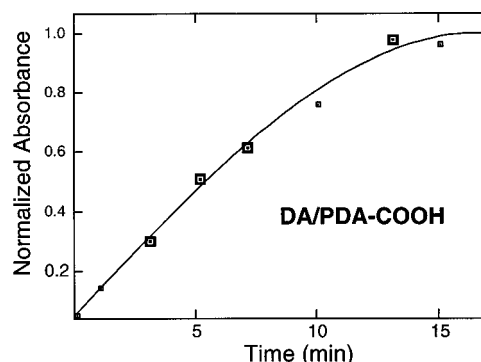
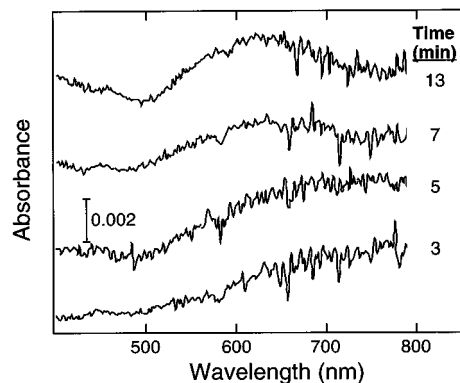


Figure 7. (Top) Transmission UV-vis spectra of partially and fully polymerized, acid-terminated DA SAMs confined to semitransparent Au thin films. UV-vis spectra are shown for UV illumination times of 3, 5, 7, and 13 min. (Bottom) Absorbance (at λ_{max}) normalized to the absorbance measured for a fully polymerized film vs irradiation time for the acid-terminated DA SAM. The data points represented by large boxes correspond to the spectra shown at the top of the figure, and the small boxes correspond to spectra (not shown) obtained at intermediate times.

Figure 8 shows analogous spectral data for a DA/PDA-OH SAM. The results are strikingly similar to those shown for the DA/PDA-COOH SAM in Figure 7. For example, λ_{max} is present around 620 nm, and the polymer remains blue even after extended UV illumination. The only notable difference between the acid- and hydroxyl-terminated materials is that the latter polymerizes somewhat more quickly: no change in the absorbance at λ_{max} is observed after 7 min.

Electrochemical Methods. Electrochemical methods have often been used as a convenient and highly sensitive means for examining the packing quality and number of defects within SAMs.^{46,59} There are two electrochemical approaches in common use for evaluating the mass-transfer-inhibiting properties of SAMs: the first is based on capacitive measurements, and the second on Faradaic processes.

When an electrochemical interface is approximated as a parallel plate capacitor, its capacitance per unit area (C) is given by eq 2, where ϵ is the dielectric constant of

$$C = \epsilon\epsilon_0/d_{\text{eff}} \quad (2)$$

the film, ϵ_0 is the permittivity of free space, and d_{eff} is the effective thickness of the SAM.^{60,61} For an impermeable barrier, d_{eff} is simply the thickness of the SAM (bottom of Scheme 4). However, if ions are able to penetrate through the SAM (top of Scheme 4), then d_{eff} is reduced and C increases. Thus, the magnitude of C , which is easily measured by cyclic voltammetry,⁶¹ is a direct measure of

(57) Kuriyama, K.; Kikuchi, H.; Kajiyama, T. *Langmuir* **1996**, *12*, 2283.

(58) Tieke, B.; Lieser, G. *J. Colloid Interface Sci.* **1988**, *2*, 471.

(59) Chailapakul, O.; Crooks, R. M. *Langmuir* **1993**, *9*, 884.

(60) Chidsey, C. E. D.; Loiacono, D. N. *Langmuir* **1990**, *6*, 682.

(61) Bard, A. J.; Faulkner, L. R. *Electrochemical Methods*; Wiley: New York, 1980; pp 10–14.

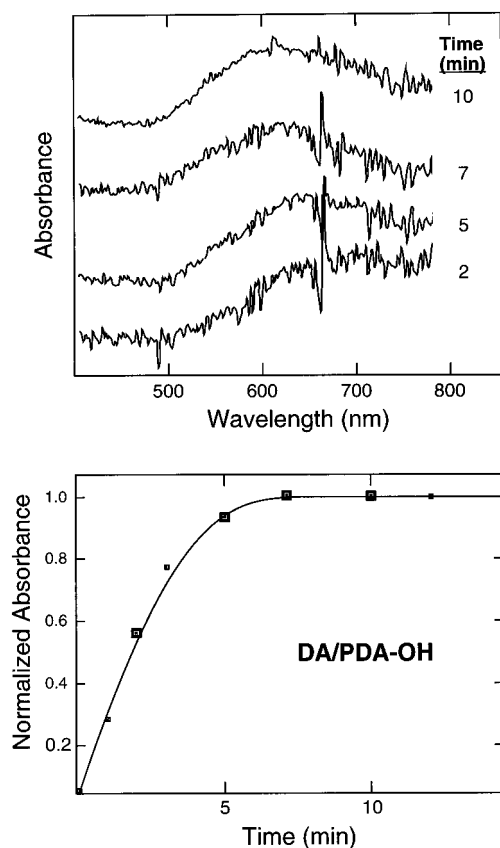


Figure 8. (Top) Transmission UV-vis spectra of partially and fully polymerized, hydroxyl-terminated DA SAMs confined to semitransparent Au thin films. UV-vis spectra are shown for UV illumination times of 2, 5, 7, and 10 min. (Bottom) Absorbance (at λ_{\max}) normalized to the absorbance measured for a fully polymerized film vs irradiation time for the hydroxyl-terminated DA SAM. The data points represented by large boxes correspond to the spectra shown at the top of the figure, and the small boxes correspond to spectra (not shown) obtained at intermediate times.

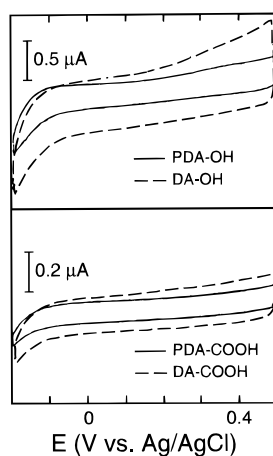
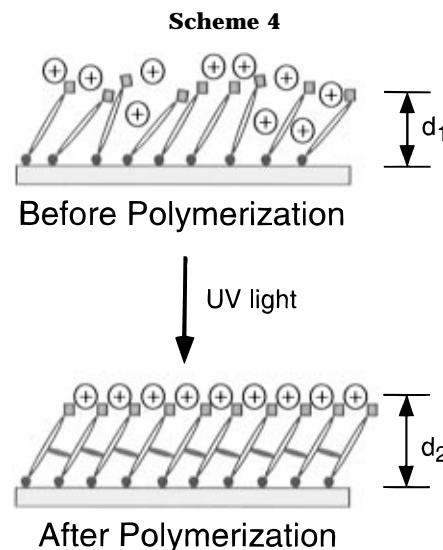


Figure 9. Double-layer capacitance measurements for hydroxyl- (top) and acid- (bottom) terminated diacetylenic SAMs. The dashed and solid lines refer to the SAMs before and after polymerization, respectively. Conditions: electrolyte solution, aqueous 0.1 M KCl; scan rate = 100 mV/s; active electrode area, 0.70 cm².

the extent to which the electrolyte penetrates the SAM. There is one potential complication to this approach when it is used for comparing diacetylenic SAMs before and after polymerization. If the thickness of the SAM changes as a result of polymerization, then d_{eff} will change and the correlation between changes in capacitive current and defect density will be compromised. However, as discussed



earlier, the thicknesses of the diacetylenic SAMs used here are unaffected by polymerization.

Figure 9 illustrates the results of the capacitive approach for evaluating the barrier properties of hydroxyl- and acid-terminated SAMs before and after polymerization.⁶⁰ The voltammograms were obtained in a potential region where little Faradaic current flows, and the capacitive current was measured in the region around 0 V, where Faradaic processes are minimal and the current is not potential dependent. The measured double-layer capacitance of DA-OH is 4.9 $\mu\text{F}/\text{cm}^2$, which is substantially higher than the capacitance of a much shorter hydroxyl-terminated *n*-alkanethiol SAM comprised of HS(CH₂)₁₀CH₂OH (<2 $\mu\text{F}/\text{cm}^2$).⁶³ This result almost certainly reflects structural deficiencies in DA-OH SAMs. The capacitance of the DA-OH SAM decreases monotonically until polymerization is complete and the capacitance reaches a constant minimum value of 2.2 $\mu\text{F}/\text{cm}^2$. The important point is that PDA-OH is a significantly better mass transfer barrier than DA-OH, which is consistent with the FTIR-ERS and UV-vis data and implies that photopolymerization serves to improve the structural and barrier properties of the monolayer. We speculate that the principal reason for this observation is that defects within DA SAMs are dynamic, and while their average size is fixed, the standard deviation of the pore size is fairly large, which leads to significant ion penetration of the film. Following polymerization, however, the films are much more rigid,⁴ and while the average pore size may not decrease, the time-dependent variation is smaller, which leads to a reduction in the average depth of ion penetration.

The capacitance of the DA-COOH SAM (1.3 $\mu\text{F}/\text{cm}^2$) is substantially lower than that of the DA-OH SAM and is approximately the same as that for the HS(CH₂)₁₀COOH SAM (~ 3 $\mu\text{F}/\text{cm}^2$) after correcting for the thickness difference in d_{eff} .⁶⁰ Following 10 min of illumination, the capacitance of the DA-COOH SAM decreased to 0.8 $\mu\text{F}/\text{cm}^2$, which is as low as that of a very good methyl-terminated SAM.⁶⁰ As observed for the DA-OH/PDA-OH system, the capacitance decreases monotonically as a function of illumination time until the SAM is fully polymerized. As discussed earlier, the lower capacitance reflects a decrease in ion penetrability arising from film stiffening and possibly increased ordering. Since the DA-OH and DA-COOH molecules are the same except for their end-group functionality, we speculate that the large differences between the capacitances of the acid- and

(62) Sabatani, E.; Rubinstein, I. *J. Phys. Chem.* **1987**, *91*, 6663.

(63) Bilewicz, R.; Majda, M. *J. Am. Chem. Soc.* **1991**, *113*, 5464.

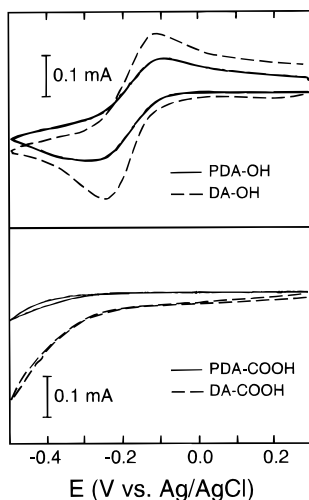


Figure 10. Cyclic voltammograms corresponding to $\text{Ru}(\text{NH}_3)_6^{3+}$ permeability through hydroxyl- (top) and acid- (bottom) terminated diacetylenic SAMs. The dashed and solid lines refer to the SAMs before and after polymerization, respectively. Conditions: electrolyte solution, aqueous 0.1 M KCl plus 5 mM $\text{Ru}(\text{NH}_3)_6\text{Cl}_3$; scan rate = 50 mV/s; active electrode area, 0.70 cm^2 .

hydroxy-terminated SAMs reflect differences in end group structure perhaps resulting from intramonolayer hydrogen bonding.

In addition to capacitive measurements, it is also possible to evaluate defects within SAMs using Faradaic electrochemistry. In this experiment, a SAM-coated Au substrate is immersed in an electrolyte solution containing redox-active probe molecules. Depending on the size and chemical nature of the probe molecules and the nanoscopic structure of the SAM, the probe molecules may completely or partially penetrate the SAM and undergo electron transfer with the Au substrate. Three possible modes of interaction are possible. First, if there are many defects within the SAM that permit probe molecules to exchange electrons with the underlying substrate, then the resulting cyclic voltammetric response will appear peak-shaped.^{46,59} This is a consequence of linear diffusion of the probe molecule to the substrate. Second, if there is a low density of micron- or nanometer-scale defects, then each defect will behave as a single ultramicroelectrode.^{59,62,63} Diffusion to individual electrodes will be radial, and as long as they are spaced sufficiently far apart that their diffusion layers do not overlap; the resulting cyclic voltammetric response will appear plateau-shaped at potentials much past E^0 .⁵⁹ Third, if there are no defect sites through which probe molecules can completely or partially penetrate, their average point of closest approach to the electrode will be roughly defined by the average thickness of the monolayer.^{64–66} In this case it may be possible to observe very small tunneling currents between the substrate and probe, which will result in cyclic voltammograms characterized by an exponential increase in current.

Interpretation of results from cyclic voltammetric experiments is most straightforward for SAMs that contain monodispersed nanometer- to micron-scale defects

that are regularly spaced and sufficiently far apart that their diffusion layers do not overlap. In this case it is sometimes possible to determine detailed structural information about defects such as their number density and size; however, this situation is never realized experimentally. Interpretation is further complicated because the cyclic voltammetric response depends on the size, shape, and charge of the solution-phase probe molecule.⁵⁹ Thus, electrochemical methods are best used for *comparing* the average properties of SAMs or other thin films rather than attempting to determine absolute defect configurations.

The cyclic voltammetric data shown in Figure 10 were obtained using exactly the same SAM-modified electrodes that were used for the capacitance measurements described earlier. For these experiments the aqueous electrolyte solution contained 5 mM $\text{Ru}(\text{NH}_3)_6^{3+}$ and 0.1 M KCl. Comparing first the relative penetrability of the hydroxyl- and acid-terminated SAMs, we find that the results mirror those obtained from the capacitance measurements: the hydroxyl-terminated SAMs are more permeable than the acid-terminated monolayers. We also find that there is a substantial decrease in probe penetration upon polymerization for both the DA-OH/PDA-OH and DA-COOH/PDA-COOH systems. On the basis of these results, the PDA-COOH SAM resists $\text{Ru}(\text{NH}_3)_6^{3+}$ mass transfer at least as well as typical methyl-terminated *n*-alkanethiol SAMs.⁵⁹

Summary and Conclusions

We have provided a detailed characterization of monomeric and polymerized diacetylenic alkanethiol SAMs having three different end groups. The results indicate that all three DAs self-assemble onto gold substrates to yield organized monolayers and that they undergo subsequent topochemical polymerization upon exposure to UV light. As discussed in a forthcoming paper, the polymerized SAMs are far more stable than the unpolymerized DA materials or simple monomeric organomer-captans.⁷ At the present time, we are exploring additional mechanical and structural aspects of the PDAs with a view toward understanding their viscoelastic properties and the length of the individual oligomeric chains. We have also begun to integrate these materials into chemically sensitive interfaces⁶⁷ and are evaluating their adhesive properties.⁵

Acknowledgment. R.M.C. and K.C.C. gratefully acknowledge financial support from the National Science Foundation (CHE-9313441) and the Office of Naval Research. This work was also funded in part under contract from Sandia National Laboratories, supported by the U.S. Department of Energy under Contract No. DE-AC04-94AL85000. T.K. acknowledges financial support from the Hallym Academy of Sciences, Hallym University. L.S. and Q.Y. acknowledge financial support from the University of Minnesota in the form of start-up funds and a summer fellowship. R.M.C. thanks Prof. Marcetta Darensbourg for use of the UV-vis spectrometer, and L.S. thanks Prof. Kent Mann for the use of the low-pressure Hg lamp.

LA960810H

(64) Chidsey, C. E. D. *Science* **1991**, *251*, 919.

(65) Becka, A. M.; Miller, C. J. *J. Phys. Chem.* **1992**, *96*, 2657.

(66) Finklea, H. O.; Hanshew, D. D. *J. Am. Chem. Soc.* **1992**, *114*, 3173.

(67) Dermody, D. L.; Crooks, R. M.; Kim, T. *J. Am. Chem. Soc.*, in press.